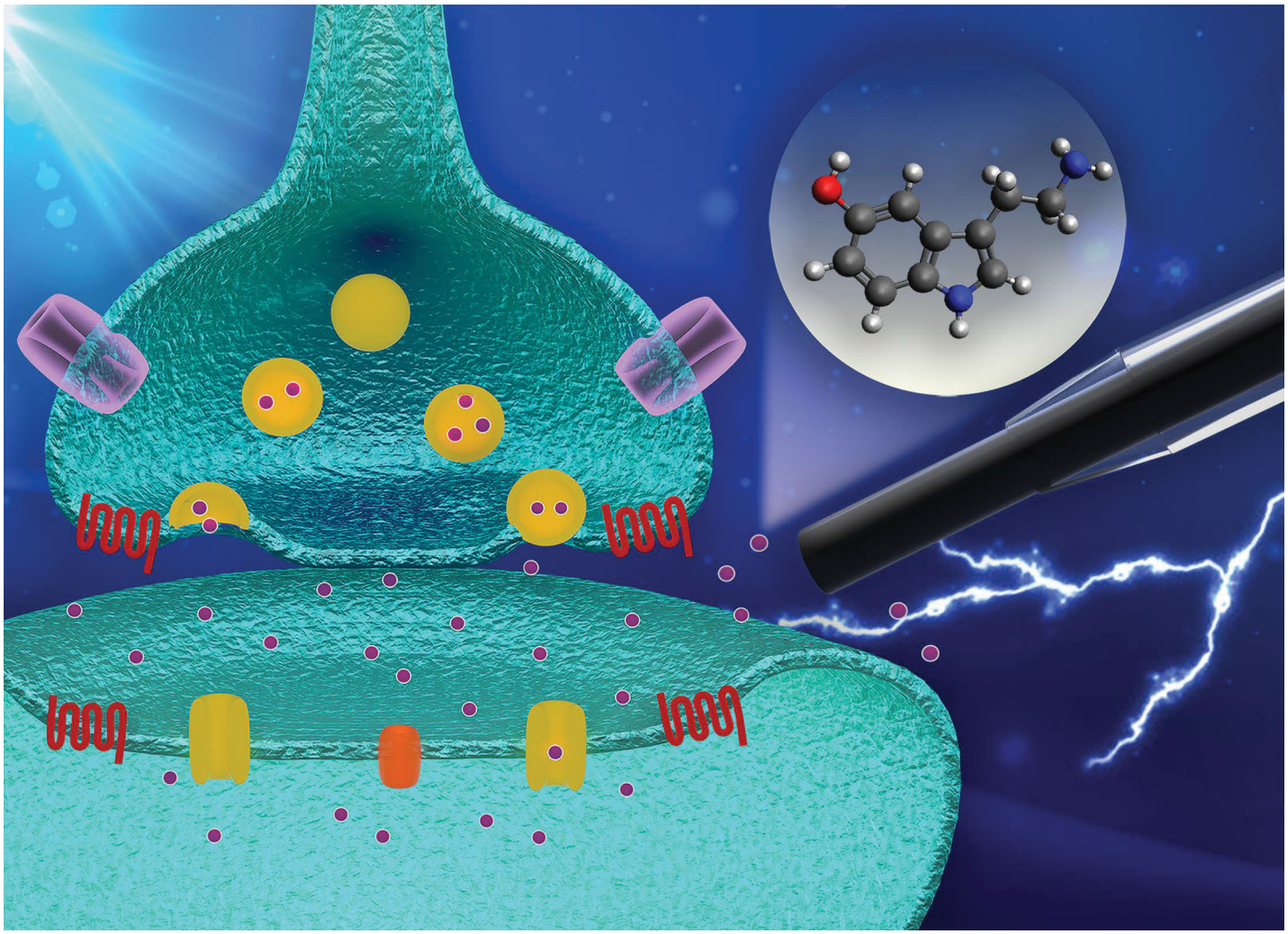

Showcasing research from Professor Ashley Ross's laboratory, Department of Chemistry, University of Cincinnati, Ohio, USA.

High Young's modulus carbon fibers are fouling resistant with fast-scan cyclic voltammetry

High Young's modulus carbon-fibers resist detrimental chemical fouling similarly to carbon nanotube fibers with fast-scan cyclic voltammetry. This provides a new method for stable detection of neurochemicals, like serotonin, without having to use costly carbon nanomaterials or complicated electrode modifications.

As featured in:

See Ashley E. Ross *et al.*, *Chem. Commun.*, 2020, **56**, 8023.

ROYAL SOCIETY OF CHEMISTRY

rsc.li/chemcomm

Registered charity number: 207890

ChemComm

ROYAL SOCIETY OF CHEMISTRY

COMMUNICATION

View Article Online
View Journal | View Issue

Cite this: *Chem. Commun.*, 2020, **56**, 8023

Received 8th April 2020,
Accepted 19th May 2020

DOI: 10.1039/d0cc02517h

rsc.li/chemcomm

High Young's modulus carbon fibers are fouling resistant with fast-scan cyclic voltammetry†

Yuxin Li, Collin M. Fleischer and Ashley E. Ross *

We report evidence that high Young's modulus carbon-fibers resist detrimental chemical fouling at their surface similarly to carbon nanotube fibers with fast-scan cyclic voltammetry. This provides a new method for stable monitoring of neurochemicals like serotonin, without the need to purchase costly carbon nanotube microfibers or perform complicated electrode immobilizations.

Fouling is a ubiquitous issue that can greatly undermine the sensitivity and stability of biosensor performance. This paper characterizes the use of high Young's modulus carbon-fibers for fouling resistant detection with fast-scan cyclic voltammetry (FSCV). FSCV is an electrochemical technique widely used to detect neurotransmitters in the brain.[1] Carbon-fiber microelectrodes are the primary electrodes used with FSCV due to their small size and excellent electrochemical properties; however, traditional carbon-fibers can be susceptible to fouling. Chemical fouling can occur from irreversible adsorption of the target analyte or of electropolymerization products on the electrode which ultimately cause significant loss in sensitivity and unstable measurements over time. Electrode surfaces which are capable of resisting chemical fouling have been developed for the electrochemical analysis field for some time.[2–4] Carbon nanotube (CNT)-based materials, highly-ordered pyrolytic graphite (HOPG),[5] and boron-doped diamond (BDD)[4,6] are prominent fouling-resistant materials in electroanalysis. A few reports have used BDD electrodes with FSCV; however, to date, BDD electrodes have not been well-adopted across the field.[6,7] Likewise, major advancements in the understanding of dopamine electrochemistry and fouling resistance at CNT-based electrodes with FSCV have been made;[8–10] however, widespread adoption of CNT materials for neurochemical detection with FSCV has not been established yet. Here, we demonstrate that high Young's modulus carbon-fibers exhibit resistance to chemical fouling, just as well as CNT-fiber electrodes. This approach provides a new method for fouling resistant detection with FSCV and beyond. By using a traditional carbon-fiber, without needing additional modifications or costly nanomaterials, we expect that this approach will be more widely adopted by the FSCV field, and more broadly to the electroanalysis field.

The mechanism of fouling resistance on materials has been well investigated for several years.[2,11,12] Several reports have demonstrated significant attenuation of the effects of serotonin fouling on CNT-based materials with FSCV.[10,13,14] We recently published a detailed investigation on the extent to which the degree of surface disorder impacts serotonin fouling on CNT-fiber based electrodes.[10] In summary, we showed that CNT-fibers which were low in surface disorder do resist chemical fouling like previously described; however, CNT-fibers which were purposefully functionalized were not resistant to chemical fouling. Despite this understanding, access to CNT microfibers can be limiting because they are not often commercially available in the diameters needed to make microelectrodes for FSCV. The diameters used for FSCV range from 5–10 μm. Using smaller fibers than this is difficult to handle for fabricating and fibers which are much larger often exhibit high capacitive current due to the fast scan rates. Oftentimes access to CNT-fibers of the correct size requires specific collaborations with groups who specialize in synthesizing CNT-based materials or customizing an order which can be quite costly.[15] These limitations may, in part, be responsible for the lack of widespread use of CNT-fibers for neurochemical detection.

Immobilizing polymers or carbon nanomaterials on the surface of carbon-fibers has been extensively used to design fouling-resistant sensors.[14,16–18] For example, Nafion is often used to coat carbon-fibers to reduce detrimental fouling from analytes such as serotonin with FSCV.[17] Additionally, composites of Nafion with poly(3,4-ethylenedioxythiopene) (PEDOT) have been electropolymerized onto the surface of carbon-fibers to improve the effects of biofouling.[16] Carbon nanomaterial-modified carbon-fiber surfaces have also been used to reduce fouling.[14,18] Although these strategies are effective, they often require lengthy fabrication steps and are not always robust. We show a cost-effective and robust carbon-fiber which exhibits similar fouling-resistant properties as CNT electrodes but don't require time-consuming electrode modifications.

University of Cincinnati, 312 College Dr, 404 Crosley Tower, OH 45221-0172, USA. E-mail: Ashley.ross@uc.edu

† Electronic supplementary information (ESI) available. See DOI: 10.1039/d0cc02517h

Young's modulus is a mechanical property that defines the stiffness of the material. In order to produce carbon-fibers with high Young's modulus, high heat treatments during graphitization, exceeding a few thousand Celsius, are necessary. High heat treatments during graphitization affect the crystallinity, molecular orientation, and lower the amount of defects on the surface.[19,20] These changes in the surface are often characterized with Raman spectroscopy.[21] Based on our previous results demonstrating that the degree of defects on the surface impacts fouling resistance of CNT materials,[10] we hypothesized that carbon-fibers with a high modulus could resist chemical fouling due to lower defects on the surface. Here, we compare the traditional carbon-fibers for FSCV detection (TS30 standard modulus, 235 GPa) to intermediate modulus (MS40, 338 GPa), and high modulus carbon-fibers (HS40, 427 GPa).

Raman spectroscopy and scanning electron microscopy (SEM) were used to characterize both quantitatively and qualitatively the surface of each fiber. Raman spectroscopy is commonly used to analyze the degree of defects on the surface of carbon-based materials. The ratio of the D band (Disorder peak, 1330–1350 cm^{-1}) and G band (graphitic peak, 1580–1590 cm^{-1}) is used to evaluate the degree of sp^3 and sp^2 hybridized carbon. High D/G ratios equates to a higher amount of defects on the carbon surface. D/G ratios were calculated by integrating the area of each peak and calculating the ratio of the areas. As expected, the high modulus carbon-fiber (HS40, Fig. 1C and Table 1) had the lowest D/G ratio. An additional peak, the 2D band (2700 cm^{-1}) is present in the Raman spectra for both MS40 and HS40 fibers (Fig. 1B and C). The 2D peak represents crystalline graphite and graphitized fibers and has been shown to become stronger and sharper as a function of fiber modulus and surface crystallinity.[22,23] The D/G ratio for TS30-fibers are significantly higher than HS40-fibers (One-way ANOVA, Bonferroni, $p < 0.0001$, $n = 6$) but not MS40-fibers ($p = 0.0666$, $n = 6$). This suggests that the change in heat treatment to produce these two different Young's moduli did significantly impact the degree of disorder on the surface; however, there are no significant differences between the degree of disorder for TS30 and MS40 fibers. The D/G ratio for the MS40-fibers are significantly higher than HS40 (One-way ANOVA, Bonferroni, $p < 0.0001$, $n = 6$). In addition, topographical differences were observed *via* SEM. The HS40-fibers were smoother than the traditional fibers (TS30) which is likely a result from the molecular orientation changes due to the increased heat treatments.

5-Hydroxytryptamine (5-HT, serotonin) is an important neurotransmitter in the brain and immune system[17] and is an analyte of interest for FSCV detection.[24] Several previous papers have demonstrated detrimental fouling by serotonin on the surface of carbon-fibers.[10,14,17] We used 5-HT as a model compound for fouling and compared the extent to which current decreases after 25 repeated injections at TS30, MS40, HS40, and pristine CNT-fiber (CNT-P) electrodes (Fig. 2A–C). The waveform applied to the electrode scanned from −0.4 V to 1.3 V at 400 V s^{-1}. Current was normalized to the first injection and plotted for each of the 25 injections (Fig. 2C). Example cyclic voltammograms (CVs) are shown for both the standard fiber (Fig. 2A) and the high modulus fiber (Fig. 2B) at the 1st and 25th injection. On average, a loss of 45 ± 3% in signal by the 25th injection was observed at TS30 fibers (Fig. 2A, $n = 12$). This

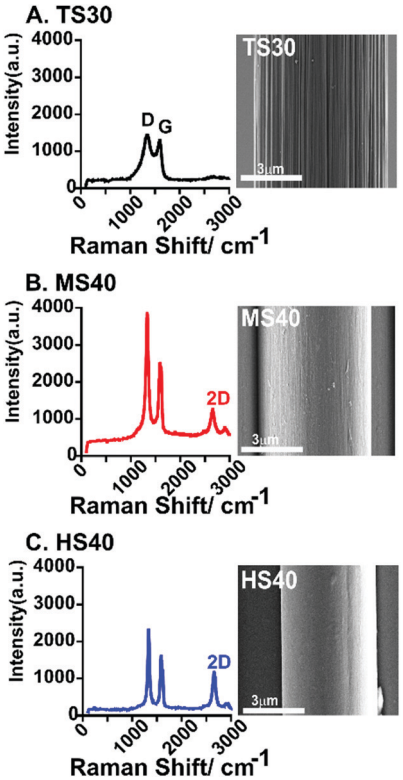

Fig. 1 Example Raman spectra of a standard modulus fiber (TS30, A), intermediate modulus fiber (MS40, B), and high modulus fiber (HS40, C). An SEM image is shown to the right of each spectra. Scale bar is 3 μm for each image. The average D/G for each fiber-type is given in Table 1.

result is comparable to similar experiments at traditional carbon-fibers.[10,13,14] In comparison, a 31 ± 3.9% loss and 26 ± 3.5% loss was observed for MS40 and HS40 fibers, respectively. The percent loss at the 25th injection between HS40 and MS40 are not significantly different (unpaired *t*-test, $p = 0.3566$, $n = 10$). A 20 ± 4.9% loss in signal was observed for the CNT-P fiber electrodes ($n = 6$). The loss in signal by the 25th injection was significantly different between the CNT-P and TS30 and between HS40 and TS30 (unpaired *t*-test, $p < 0.001$). The loss in signal was not significantly different by the 25th injection between the HS40 and CNT-P ($p > 0.05$) demonstrating that the HS40 fibers are just as good at resisting serotonin fouling as the CNT materials. The loss in signal was also not significantly different between the MS40 and CNT-P fibers ($p > 0.05$). Despite the similarity between CNT-P and MS40 fibers, the fouling resistance was less robust at these fibers, with a few fibers not exhibiting fouling resistance at all, likely because of defects on the MS40 surface. Therefore, we chose HS40 fibers as optimal for improving fouling resistance robustly.

5-Hydroxyindoleacetic acid (5-HIAA) is a major metabolite of serotonin and has been shown to foul the electrode surface. The concentration of 5-HIAA in the brain is 200–1000 times higher than 5-HT therefore it is important to have electrodes which are significantly more sensitive to 5-HT than 5-HIAA.[25] Previous work has demonstrated that Nafion coated carbon-fibers are significantly less sensitive to 5-HIAA compared to 5-HT due to the anion-exchange properties of the polymer.[17] Here, we compared the

Table 1 Comparison of electroactive surface area, sensitivity, ΔE_p, and D/G ratio for TS30, MS40, and HS40 fibers

Fiber	Diameter (μm)	Electroactive surface area[b] (cm^2)	Sensitivity (DA) (nA μM^{-1})	Sensitivity (5-HT) (nA μM^{-1})	Sensitivity (5-HIAA) (nA μM^{-1})	5-HT:5-HIAA sensitivity	ΔE_p	D/G ratio
TS30	7	1.2×10^{-3}	6.6 ± 0.6	7.5 ± 0.9	3.0 ± 0.1	2.5	0.9 ± 0.01	1.8 ± 0.2
MS40	6	2.4×10^{-4}	2.1 ± 0.1	—	—	—	0.9 ± 0.01	1.7 ± 0.1
HS40	5	1.7×10^{-4}	1.5 ± 0.1	2.8 ± 0.7	0.4 ± 0.06	7.0	0.9 ± 0.02	[a]1.3 ± 0.0****

[a] Significant difference between the D/G ratio for TS30 and HS40 fibers (One-way ANOVA, Bonferroni, $p < 0.0001$, $n = 10$). [b] Calculated error was <0.0001 cm^2.

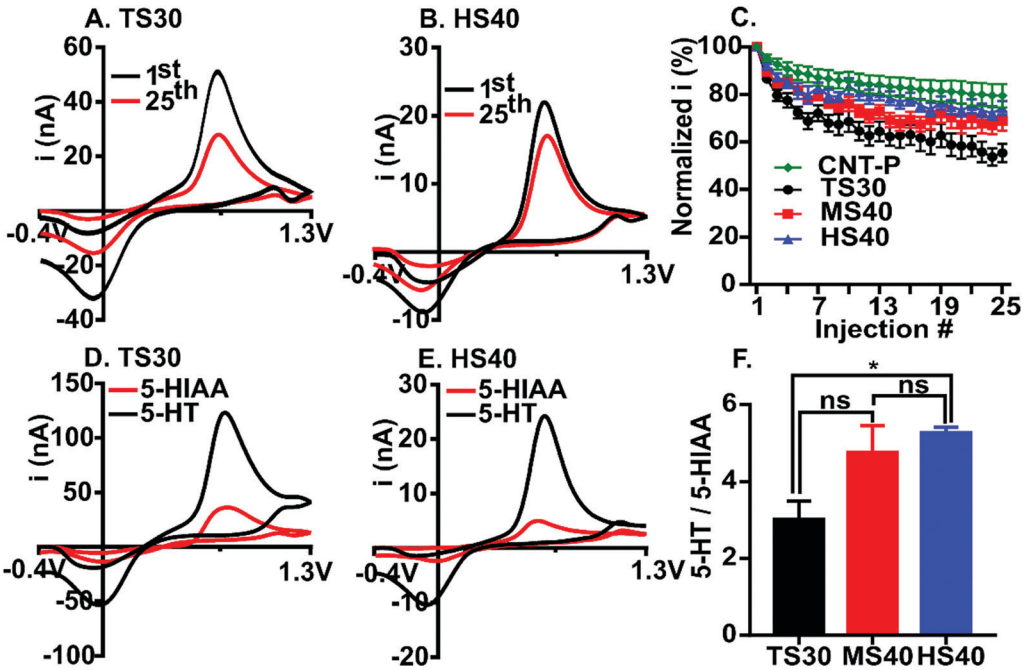

Fig. 2 High modulus fibers exhibit significantly improved fouling resistance to serotonin compared to TS30. Cyclic voltammograms of 5-HT are compared for the 1st (black) and 25th (red) injection for (A) TS30 and (B) HS40 fibers. (C) Average normalized current *vs.* injection number for all 25 injections are plotted for TS30 (black), MS40 (red), HS40 (blue) and CNT-pristine fibers (green) (n = 6–12). Current detected for 5-HT and 5-HIAA was compared for (D) TS30 and (E) HS40 fibers. (F) The average ratio of 5-HT to 5-HIAA current for TS30, MS40, and HS40 demonstrates that HS40 fibers are the least sensitive to 5-HIAA. (n = 6).

current ratio for 1 μM 5-HT to 10 μM 5-HIAA for TS30, MS40 and HS40 fibers to investigate the interaction of 5-HIAA at high modulus fibers (Fig. 2D–F). Example voltammograms comparing the current for TS30 and HS40 fibers are demonstrated in Fig. 2D and E. The ratio of 5-HT to 5-HIAA current for MS40 fibers was not significantly different than the TS30 and HS40 (One-way ANOVA, Bonferroni, TS30 $p = 0.08725$, HS40 $p > 0.9999$, $n = 6$); however, the ratio was significantly higher for HS40 compared to TS30 (One-way ANOVA, Bonferroni, $p = 0.0238$, $n = 6$). The average ratio of 1 μM 5-HT to 10 μM 5-HIAA current is 3.0 ± 0.5 for TS30, 4.8 ± 0.7 for MS40, and 5.3 ± 0.1 for HS40. This result demonstrates that HS40 fibers improved the selectivity for 5-HT over 5-HIAA by 1.8-fold. Although HS40 are more sensitive to 5-HT, Nafion coated carbon-fibers have previously demonstrated a 17.4 ± 10.3 ratio of 5-HT to 5-HIAA current at the same concentrations tested here.[17] Despite these differences, our work was done at the traditional FSCV waveform, not the "serotonin waveform[26]". This is significant because the serotonin waveform is limiting, not allowing co-detection with other analytes, and requires faster scan rates (1000 V s^{-1}). Our work provides evidence that you can improve selectivity for 5-HT over 5-HIAA at the traditional FSCV waveform, and without the need to modify the electrode surface.

Despite improvements in fouling resistance, a loss in sensitivity was observed at high modulus carbon-fibers (Fig. 3 and Table 1). Calibration curves were generated for dopamine, 5-HT, and 5-HIAA at TS30 and HS40 fibers. Previously, a waveform was developed to control the fouling of 5-HT which scans from 0.2 V to 1.0 V scan, then down to −0.1 V and back to 0.2 V, at 1000 V s^{-1}.[26] This waveform is currently the only waveform used to detect serotonin with FSCV. To compare sensitivity, we collected the calibration data for 5-HT at the "serotonin waveform" for the traditional TS30 fibers. The traditional waveform was used for the HS40 fibers because limited fouling is observed on the high modulus carbon surface. We used the traditional waveform for dopamine calibration curves at all fibers. Sensitivity for dopamine (DA) was 4.4-fold higher at the traditional TS30 fibers compared to the HS40 fibers (Fig. 3 and Table 1, n = 6–10). We suspect that this is due to two main reasons: the diameters of HS40 fibers are smaller and

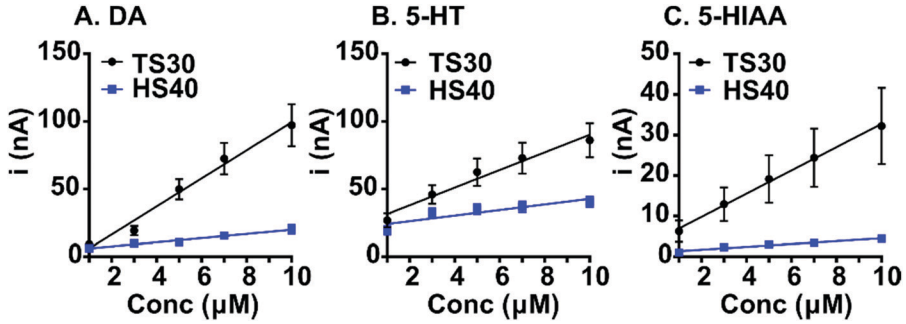

Fig. 3 Sensitivity comparison for TS30 and HS40 fibers. All calibration curves were conducted from 1 μM to 10 μM. (A) Dopamine (waveform: −0. 4 V to 1.3 V, 400 V s^{-1}, n = 6–10), (B) 5-HT, and (C) 5-HIAA (waveform for TS30: 0.2 V to 1.0 V, down to −0.1 V and back to 0.2 V, 1000 V s^{-1}; HS40: −0.4 V to 1.3 V, 400 V s^{-1}, n = 8–10).

because dopamine electrochemistry is highly surface dependent relying on surface oxides which are likely not present at less disordered surfaces.[27] Similarly to dopamine, HS40 were less sensitive to 5-HT at the traditional waveform compared to TS30 fibers at the "serotonin waveform" by 2.7-fold (Fig. 3B and Table 1). This is likely a result of the differences in scan rate between the two waveforms and electrode size. Calculated electroactive surface areas were also smaller by an order of magnitude at high modulus fibers; however, this is due to smaller currents measured at higher modulus fibers because the fibers are smaller (Table 1). Despite this finding, HS40 fibers are on average 7.5-fold less sensitive to 5-HIAA than the traditional TS30 fibers. In addition, HS40 fibers are 7.0-fold more sensitive to 5-HT than 5-HIAA, compared to only 2.5-fold more sensitive at TS30 fibers (at the traditional serotonin waveform) (Table 1). This demonstrates that a significant loss in sensitivity to 5-HIAA is capable at high-modulus fibers. Future studies could increase the scan rate for detection of serotonin at high-modulus fibers to improve serotonin sensitivity while maintaining limited fouling on the surface.

High modulus fibers have similar electron transfer rates compared to standard modulus carbon-fibers (Table 1). We calculated and compared the ΔE_p for dopamine at TS30, MS40, and HS40 fibers. This provides information on the relative rate of electron transfer at the surface. Overall, we demonstrate that increasing the modulus of the fibers, which decreases the degree of disorder on the surface, does not significantly impact the reaction rate at the electrode (One-way ANOVA, $p > 0.05$, $n = 6$).

Overall, the temperature used during graphitization of carbon fibers has dramatic effects on the electrochemical performance including fouling resistance and selectivity. The resistance to fouling and lower sensitivity to promiscuous anionic metabolites is an important finding which will have a significant impact on improving the stability of neurochemical detection with FSCV and other electroanalysis techniques. In addition, we show that high modulus carbon-fibers are capable of resisting chemical fouling just as well as CNTs. This is a key finding which will provide researchers an alternative strategy for developing robust and cost-effective fouling-resistant sensors. Thus, this work lays a framework for fine-tuning the mechanical properties for optimized electrode performance.

We would like to acknowledge Dr Noe Alvarez for gifting us carbon nanotube fibers for this study.

Conflicts of interest

The authors declare no conflicts of interest.

Notes and references

1 P. Puthongkham and B. J. Venton, *Analyst*, 2020, **145**, 1087–1102.
2 B. L. Hanssen, S. Siraj and D. K. Y. Wong, *Rev. Anal. Chem.*, 2016, **35**, 1–28.
3 W. Harreither, R. Trouillon, P. Poulin, W. Neri, A. G. Ewing and G. Safina, *Anal. Chem.*, 2013, **85**, 7447–7453.
4 R. Trouillon, Y. Einaga and M. A. M. Gijs, *Electrochem. Commun.*, 2014, **47**, 92–95.
5 F. M. Maddar, R. A. Lazenby, A. N. Patel and P. R. Unwin, *Phys. Chem. Chem. Phys.*, 2016, **18**, 26404–26411.
6 K. E. Bennet, J. R. Tomshine, H.-K. Min, F. S. Manciu, M. P. Marsh, S. B. Paek, M. L. Settell, E. N. Nicolai, C. D. Blaha, A. Z. Kouzani, S.-Y. Chang and K. H. Lee, *Front. Hum. Neurosci.*, 2016, **10**, 102.
7 K. E. Bennet, K. H. Lee, J. N. Kruchowski, S.-Y. Chang, M. P. Marsh, A. A. V. Orsow, A. Paez and F. S. Manciu, *Materials*, 2013, **6**, 5726–5741.
8 Q. Cao, D. K. Hensley, N. V. Lavrik and B. J. Venton, *Carbon*, 2019, **155**, 250–257.
9 A. C. Schmidt, X. Wang, Y. Zhu and L. A. Sombers, *ACS Nano*, 2013, **7**, 7864–7873.
10 M. E. Weese, R. A. Krevh, Y. Li, N. T. Alvarez and A. E. Ross, *ACS Sens.*, 2019, **4**, 1001–1007.
11 S. Chandra, A. D. Miller, A. Bendavid, P. J. Martin and D. K. Y. Wong, *Anal. Chem.*, 2014, **86**, 2443–2450.
12 X. Sun, J. Wu, Z. Chen, X. Su and B. J. Hinds, *Adv. Funct. Mater.*, 2013, **23**, 1500–1506.
13 A. G. Zestos, C. B. Jacobs, E. Trikantzopoulos, A. E. Ross and B. J. Venton, *Anal. Chem.*, 2014, **86**, 8568–8575.
14 B. E. K. Swamy and B. J. Venton, *Analyst*, 2007, **132**, 876–884.
15 C. Yang, E. Trikantzopoulos, C. B. Jacobs and B. J. Venton, *Anal. Chim. Acta*, 2017, **965**, 1–8.
16 R. F. Vreeland, C. W. Atcherley, W. S. Russell, J. Y. Xie, D. Lu, N. D. Laude, F. Porreca and M. L. Heien, *Anal. Chem.*, 2015, **87**, 2600–2607.
17 P. Hashemi, E. C. Dankoski, J. Petrovic, R. B. Keithley and R. M. Wightman, *Anal. Chem.*, 2009, **81**, 9462–9471.
18 P. Puthongkham and B. J. Venton, *ACS Sens.*, 2019, **4**, 2403–2411.
19 X. Huang, *Materials*, 2009, **2**, 2369–2403.
20 J.-S. Tsai and C. J. Wu, *J. Mater. Sci. Lett.*, 1994, **13**, 272–274.
21 H. Serizawa, S. Sato, H. Tsunakawa and A. Kohyama, *TANSO*, 1997, 8–13.
22 N. Melanitis, P. L. Tetlow and C. Galiotis, *J. Mater. Sci.*, 1996, **31**, 851–860.
23 X. Qian, X. Wang, J. Zhong, J. Zhi, F. Heng, Y. Zhang and S. Song, *J. Raman Spectrosc.*, 2019, **50**, 665–673.
24 R. A. Saylor, M. Hersey, A. West, A. M. Buchanan, S. N. Berger, H. F. Nijhout, M. C. Reed, J. Best and P. Hashemi, *Front. Neurosci.*, 2019, **13**, 362.
25 A. Zangen, D. H. Overstreet and G. Yadid, *J. Neurochem.*, 1997, **69**, 2477–2483.
26 B. P. Jackson, S. M. Dietz and R. M. Wightman, *Anal. Chem.*, 1995, **67**, 1115–1120.
27 J. G. Roberts, B. P. Moody, G. S. McCarty and L. A. Sombers, *Langmuir*, 2010, **26**, 9116–9122.

